NEW MEASUREMENT TECHNIQUES IN THE ONERA LARGE WIND TUNNELS

Jean-Marc Bousquet, Marianne Lyonnet, André Mignosi
ONERA, Computing, Engineering and Testing Facilities, France
tel.: 33-1-46734230, fax: 33-1-46734144, email: bousquet@onera.fr

Keywords: *Measurement techniques, Wind Tunnels, Aerodynamics.*

Abstract

This paper presents recent achievements made in the ONERA large wind tunnels in using new measurement technique, which allow an improved flow characterization while keeping the wind tunnel productivity high. The developments concern both surface measurement techniques (as PSP Pressure Sensitive Paints) and flowfield measurement techniques (as PIV Particle Images Velocimetry, and DGV Doppler Global Velocimetry). In all the cases, a detailed validation of the new techniques is made by comparison with known techniques before application to industrial tests.

1. Introduction

ONERA's large industrial wind tunnels are located principally at two sites in France. The Centre of Modane-Avrieux, in the French Alps, is home of the S1MA subsonic/transonic wind tunnel, and the S2MA transonic/supersonic wind tunnel, with supporting S4B and BD2 test rigs, primarily for engine studies. The Centre of Le Fauga-Mauzac, South-West of Toulouse, is home of the large, high Reynolds number, low-speed F1 wind tunnel, and of some smaller research wind tunnels, as F2 dedicated to optical measurement techniques applications. There is also an anechoic CEPRA19 wind tunnel in Saclay, near Paris. A scope of the capabilities available in our wind tunnels may be found in references [1] and [2] , or on www.onera.fr/gmt-en .

With the objective to better satisfy our traditional customers and attract new clients, a continuous effort is made in improving and developing new test capabilities. For this purpose, our measurement teams in both Modane and Le Fauga centers have established deep contacts with the specialized teams working in the different research departments of ONERA. This close relationship allows the transfer of information from the scientists to the operators, and offers the opportunity to check that new techniques or technologies which are claimed to be operational in the laboratory may be used in an efficient manner in the large wind tunnels.

The present paper gives an overview of how we improve the aerodynamic measurement techniques available in our large wind tunnels in order to meet the future needs of the global aerospace business.

2. Measurements on model surface by pressure sensitive paints (PSP)

In the Modane Center, the PSP technique is regularly used for industrial tests in the transonic wind tunnels (see applications on a nacelle and a wing in S2MA, and on a missile fin in S3MA on figure 1). The principle of the intensity method used at ONERA [3] is based on the characteristics of luminescent compounds which, when illuminated by an appropriate light source, re-emit light inversely proportional to the pressure P and directly proportional to the excitation light intensity and to the luminescent component concentration in the paint. The excitation light and thickness effects are suppressed by computing the pressure field from the ratio of two images, one recorded wind-off at known conditions, and the other recorded wind on at unknown conditions.

To account for the variations during a test of the distance between the model and the light source, we use a binary paint, originally the Russian B1 paint and now the ONERA ON1 paint. The luminescence of the first component depends significantly on the air pressure, which is not the case of the second component which can be used as a reference channel to compensate for variations of the excitation light intensity. When excited by UV light (around 340nm), the pressure sensitive component emits in blue region around 450 nm, while the insensitive one emits in red region, over 620 nm (figure 2).

Recording two run images, one with a blue filter, the other with a red filter, and using the ratio Iblue/Ired enables the excitation effect to be removed. However, it is still necessary to normalise this ratio by the value Iblue/Ired obtained from the wind off image (figure 3).

2.1. Calibration and corrections

The calibration of the PSP paint is performed before the test using small samples painted at the same time as the model and installed in a vessel with pressure and temperature control (pressure range 0.1 bar to 4 bar, temperature range –10°C to +60°C).

The calibration laws deduced from the sample tests are checked on the real model where the thickness of the paint may be not constant, either in the wind tunnel by varying the pressure wind-off or now in a dedicated tank. For some models it was noted that local sensitivity differences, in particular areas like leading edge, could result in pressure differences as high as +/- 2000Pa (figure 4). An additional correction is so applied for each pixel as a function of pressure.

Deformations of the model during test are taken into account through the red image which enables to correct the model displacement in the illumination field. However, the model deformation itself can induce significant errors as the grid which is used to realign wind-on and wind-off images and to extract the results, is deformed. A specific module of the Afix2 data processing software developed by the ONERA DAFE department [4] allows the additional account of specific markers position to correct for this effect as shown on figure 5. In general, the deformation correction modifies significantly the pressure distribution in the wing tip area where this effect is important (figure 6).

2.2. Applications of PSP

The PSP technique is used as a routine technique in the transonic test section of S2MA since 1994 for research applications as well as industrial tests. One example is given on figure 7, where the PSP measured pressure distribution on the upper side of a commercial aircraft wing is compared to pressure taps results measured with PSI transducers; the agreement of both methods is very good in these cruise conditions.

Recently, the method has been extended to measure the whole aircraft pressure distribution during the same run by the so-called “360° technique”. For this, one uses 4 cooled CCD cameras (3 Princeton VersArray 1024x1024 pixels; and 1 Princeton VersArray 1340x1300 pixels) mounted in floor, ceiling and one sidewall (see figure 8). Illumination is made by 4 Hamamatsu L8222-02 UV lamps, each connected to 2 fiber-optic light sources. These 8 light sources are distributed 3 in the ceiling; 2 in the floor; and 3 in the sidewall.

As shown on figure 9, the “360° technique” was applied on a Generic Biz-Jet model coated with the new ON1 PSP paint. The Afix2 software has been used to reconstruct the full pressure distribution on the aircraft from the 4 cameras images, with account of wide-angle lenses deformation corrections. In this first application, the left side of the model was not fully illuminated and flow symmetry was assumed in post processing the data.

Application of the PSP technique in the large S1MA wind tunnel environment is more severe as it is necessary to illuminate the model placed at least 4 meters from the light source, to protect the measurement devices from the vibrations transmitted by the wind tunnel and to take account of the disruptive effect of

temperature (which can reach 60°C in the tunnel) and luminosity (which depends on the time of the day)

As shown on figure 10, special arrangements are made to take account of the specific characteristics of the wind tunnel. A Nitrogen impulse laser was installed on the ceiling of the wind tunnel cart. Two 512x512 Princeton CCD cameras, back illuminated, cooled at –45°C and with 16 bit resolution were used for image acquisition. Each camera was equipped with a switchable red/blue filter; with the lens selected for the camera located behind the wind tunnel floor the resolution is about 0.8 mm per pixel. An example of pressure field image computed from PSP images is shown in figure 11 in the region of the wing/mast/nacelle junction which is difficult to equip with pressure taps.

A comparison of PSP results with pressure tap measurements is made on figure 12 for cruise Mach number conditions. Maximum deviations are lower than 0.04 in Cp and standard deviation is less than 0.02. These values are representative of the repeatability obtained in the complete range of Mach number from 0.7 to 0.84.

Recently, PSP technology was used in S1MA in order to confirm hinge moment measurements obtained on the rudder of an Airbus model. Images of pressure field measured on both sides of the fin are presented in figure 13. A comparison of hinge moment obtained from local balance or PSP integration is presented in figure 14, on both the upper and lower part of the rudder. The agreement between the 2 measurements is very satisfactory, better than 0.01 in CMC.

Application of PSP in supersonics has been made in the S3MA blow-down wind tunnel (section 0.8mx0.8m). The study presented here concerns the control of missile configurations using lateral supersonic jets. This model was equipped with 2 lateral nozzles fitted by high pressure air. The interaction of these 2 jets with the external flow creates a complex pressure distribution on the model for which the PSP technology is particularly well adapted. The PSP images were acquired for 2 different positions of the model roll angle and grouped together to determine the complete pressure field on the model. Pressure distributions obtained at Mach 2.0, Alpha=0° and mapped on the grid are presented in figure 15 for 2 values of pressure ratio. A comparison with pressure tap values is presented in figure 16 with and without pixel by pixel calibration. The agreement between PSP and the reference pressure measurements is good, the use of pixel by pixel calibration improving slightly the PSP accuracy.

For low speed and high pressure flows, the application of the PSP technique is more challenging, and is still in development. In fact, at low velocities, the PSP measurements require the utmost accuracy which the paint can deliver, typically better than one thousandth for Mach numbers lower than 0.3; in addition, at high pressure, the light emission can be almost completely inhibited by the oxygen. As an example, figure 17 shows the results of a swept half-wing test in the pressurized F1 wind tunnel in Le Fauga at M=0.25. The PSP results are quite satisfactory over the central part of the wing, as indicated by the comparison of PSP and PSI measurements (figure 18). On the slats and the flaps, some discrepancies appear that are probably due to the camera orientation with respect to those surfaces. The improvement of the PSP technique in these low speed and high pressure flows is currently one of the major objectives of the technical development studies in the ONERA wind tunnels.

3. Flowfield measurement techniques

Many flowfield measurements techniques are developed in the Onera research departments. In order to select the best technique to install in the GMT large wind tunnels, an exhaustive analysis has been conducted in the F1 wind tunnel to compare the respective merits of the five holes probe, the DGV and the PIV techniques by performing a flow survey in the wake of a civil aircraft wing (figure 19) [5].

3.1. Doppler Global Velocimetry (DGV)

The Doppler Global Velocimetry is a planar velocimetry technique based on the Doppler effect, to measure the 3 components of the velocity field. The measurement area is materialized by a laser sheet; the light scattered by seeding particles is frequency-shifted with regard to the incident light [6]. An iodine cell is used to convert frequency to intensity, enabling bidimensional measurement with CCD cameras.

The general arrangement of a DGV receiving box (left side of figure 20) includes a pair of cooled 12-bit CCD cameras (1376 x 1024 pixel spatial resolution). The so-called "signal image" is obtained by viewing through the iodine cell, whereas the reference image is the raw image of the field. These two images are optically superposed with account of the Mie scattering which depends on viewing angle. The residual misalignment is compensated by the data processing software during the calibration steps.

At least three Doppler maps are necessary to solve the three velocity components. In our case, it was chosen to use 2 receiving boxes and 2 light sheets which were activated successively, the data processing software being able to solve the redundant information.

Calibration of the iodine cell is made by the DEFI device (Frequency to Intensity Calibration Device) which was designed and patented at ONERA. The principle relies on the observation of known-frequency light sources, which can be analyzed between each image acquisition during the course of experiments; a rotating mirror piloted by the software switches from one mode to the other.

The whole optical system is calibrated before the test by setting a calibration grid in the wind tunnel, in order to correlate the $\vec{R}$ and $\vec{E}$ unit vectors representing the observation direction (from particle to receiver) and the incident light direction (from laser source to particle) defined in the Doppler equation, with the wind tunnel coordinates. These calibration steps are quite automated and quick to perform.

In this experiment, seeding of the flow was performed with a Laskin Nozzle which generates micronic olive oil droplets.

As shown on figure 21 in a plane located at 0.5 span downstream of the wing of the civil aircraft (figure 19), the measured Doppler maps detail very precisely the wakes of the wing different components, the gray level being mainly proportional to the axial velocity component V_X. One notices from right to left on the photos, the wing/fuselage junction vortex, then the aileron contra rotating vortices, the flap vortices and the wing tip vortex. The flow structure description is very similar to the one deduced from classical 5 holes probe measurements (figure 21, left); the global comparison of the measurements shows a good agreement of the three components of the velocity field between the two techniques (figure 22).

When analyzing more in detail, one notices on figure 23 that the gradients of velocity are rather smoothed out when passing through the vortex. The theoretical accuracy of 1 or 2 m/s for DGV is not achieved here, where differences up to 5m/s being noted between DGV and pressure tap measurements. In complement, application of the DGV method in F1 showed that stray light suppression may be a challenge, and that the DGV technique requires a high degree of seeding in the flow.

3.2. Particle Images Velocimetry (PIV)

The principle of Particles Images Velocimetry (PIV) is based on the direct determination of the two fundamental dimensions of the velocity: length and time. Using a light sheet, a double pulsed laser beam illuminates twice within a short time interval the particles seeded in the flow. Measure of all three components of the velocity vector (technique called 3C PIV) is achieved by using a stereoscopic approach which consists in observing the laser light sheet from two different viewing axes, as illustrated on figure 24.

The PIV method has been applied on the same civil aircraft configuration presented on figure 19.

In this test, the light source is a compact pulsed Nd:YAG laser with dual oscillator manufactured by Quantel, supplying two consecutive pulses at 10 Hertz. Each pulse duration is about 10 ns. The light wavelength is 532 nm (green).

The tracer particles are generated by a cylindrical container with six Laskin nozzles. This generator produces large quantities of olive oil droplets of approximately 1 µm in diameter.

For the recording of PIV images, two high-resolution cooled digital 12-bit CCD cameras (1376 x 1040 pixels) are used. Each camera is equipped with a 105mm f/5.6 lens which focus is motorized. The laser and the cameras are synchronized.

The measured velocities (typical velocity map plotted on figure 25) are in very good agreement with 5 holes probe measurements and DGV measurements.

Figure 26 shows a comparison of velocity measurements made through the vortex, as measured by PIV and 5 holes probes. One notices that the velocity gradients are also smoothed in the PIV measurement by comparison with the 5 holes probe measurement, in particular on the V_Z component. The difference between the two methods is of the order of 4m/s. In consequence, the accuracy is of the same order as the DGV accuracy during this experiment, as mentioned in paragraph 3.1. Nevertheless, the application of the PIV technique appears easier in the large wind tunnel environment than the DGV technique, with less seeding required.

3.3. PIV applications for unsteady flows

The PIV technique has also been used in the F1 wind tunnel to characterize the wake of a helicopter model (as illustrated on figure 27) [7], by synchronizing the PIV image acquisition with the rotor position in azimuth.

The measurements made in different planes (either with the 2 components or the 3 components strategies) detail precisely the wakes of each of the blades (figure 28). The PIV acquisition performed at 64 different positions of the main rotor blades are currently used for validation of 3D unsteady Navier Stokes computations. It has been concluded from these different studies that the PIV method is mature for use during industrial tests in the F1 low speed wind tunnel.

3.4. Flowfield measurements : perspectives

As stated in the comparison of DGV and PIV techniques, the choice has been made to purchase a dedicated 3 components PIV system, which can be moved from one wind-tunnel to the other, depending on the test requirements.

The laser source is a QUANTEL Brilliant B pulsed 3 W Nd:YAG laser pair with two consecutive 380 mJ pulses provided at up to 7 Hz. The two cameras are LaVision (PCO 2000) Imager Pro Plus type (4 Mpixel). As illustrated in figure 29, the system has been already used in the transonic S2MA wind tunnel where a DEHS seeding apparatus was installed upstream of the test section and in the anechoic CEPRA19 wind tunnel where a DEHS seeding device is installed on demand.

4. Conclusion

The present overview has shown how the measurements techniques are continuously improved in our large wind tunnels, in order to better analyze the details of the aerodynamic behavior of the tested vehicles.

The Pressure Sensitive Paint technique has reached a high level of maturity, and can be used in most of the Onera wind tunnels with a sufficiently high accuracy to replace at least parts of the pressure tap instrumentation on the aircraft model. Although this technique is not yet fully operational in the low speed wind tunnels, this capability should be available soon as it is currently worked on in our development plans.

The detailed analysis of the flowfield is performed with the PIV technique. The high

accuracy of this technique was demonstrated by comparison with more classical five-hole probes results. This technique may be also used for the unsteady characterization, as it was made on a helicopter wake in the F1 low-speed tunnel. In complement, the high capacities of the recently acquired PIV system have been demonstrated in the transonic S2MA wind tunnel and in the CEPRA19 anechoic wind tunnel.

For more specific cases, the DGV technique has shown to be a powerful tool, as demonstrated by comparison with five holes probes and PIV results.

More generally, the new aerodynamic measurement techniques now available in our large wind tunnels are ready to meet the future needs of the global aerospace business, which is of high importance for CFD code validation and for development of new technologies to improve aerospace efficiencies.

References

[1] Wolf S., Prieur J., Bècle JP., Wagner P., Quémard C., An updated overview of wind tunnel testing capabilities for civil aircraft development in the Large Industrial Wind Tunnels of ONERA, *CASI 48th Annual Conference, April 2001*, Toronto. *(also ONERA TP2001-97)*

[2] Bousquet JM., Survey of Engine Integration Testing in ONERA Wind Tunnels, AIAA 2005-3705

[3] Lyonnet M., Fargier T., Deléglise B., Sonnet D., PSP Application in the ONERA GMT Wind Tunnels, AG37GARTEUR Report, ONERA TR4/08811DTEX

[4] Lyonnet M., Deléglise B., Lesant Y., Application of Pressure Sensitive Paint Technique in the S1MA Wind Tunnel, AIAA 2002-0744

[5] Mignosi A., Lempereur C., Barricau P., Gleyzes C., Monnier JC., Gilliot A., Geiler G., Development of optical flow field measurement techniques in the ONERA F1 low-speed wind tunnel. *ICIASF Conference*, Japan, sept. 2005.

[6] Willert C., Lempereur C., Barricau P., Wernert P., Martinez B., Applications of DGV in transonic and supersonic wind tunnels, *VKI Lecture Series Advanced Measurement Techniques for Supersonic Flows* Feb 28-March 03, 2005

[7] Le Pape A., Gatard J., Monnier JC, Experimental Investigations of Rotor-Fuselage Aerodynamic Interactions using a helicopter Powered Model, *30th European Rotorcraft Forum*, Marseilles, 14-16 September 2004.

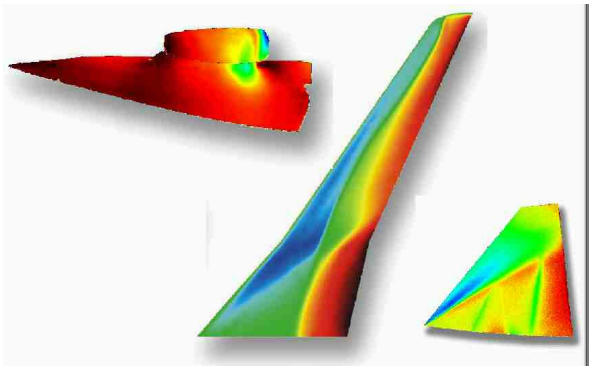

Fig 1: PSP measurements in transonic : nacelle & wing in S2MA (left & middle) ; missile fin in S3MA (right)

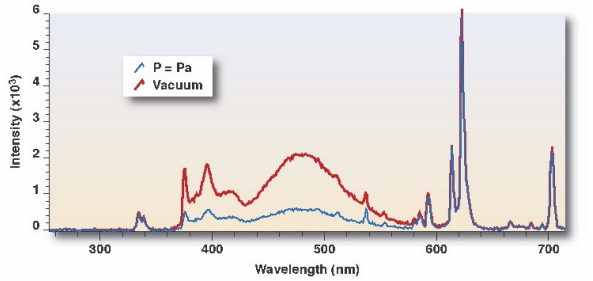

Fig. 2:Pressure spectrum of 2 components PSP paint

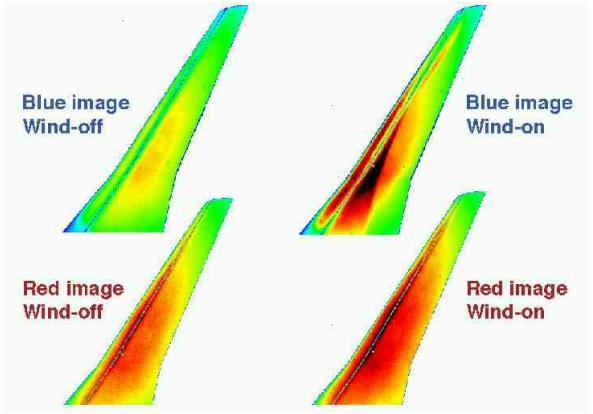

Fig. 3: PSP measurements : data acquisition with 2 component paint

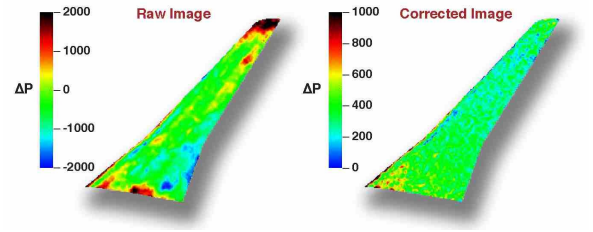

Fig. 4:PSP measurements : pixel by pixel correction

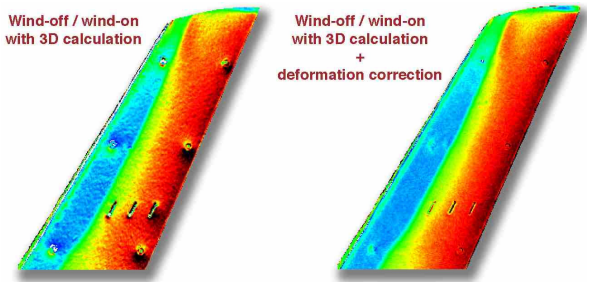

Fig. 5: PSP measurements : deformation effect on pressure field

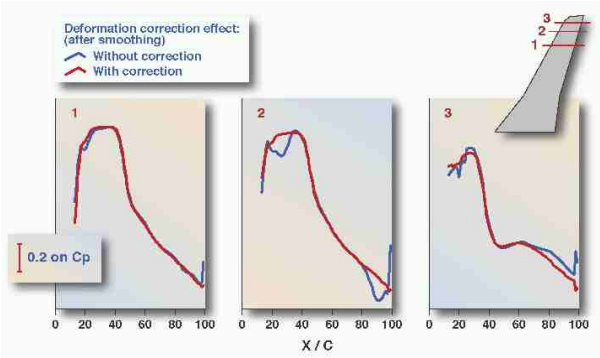

Fig. 6: PSP measurements : deformation correction effect

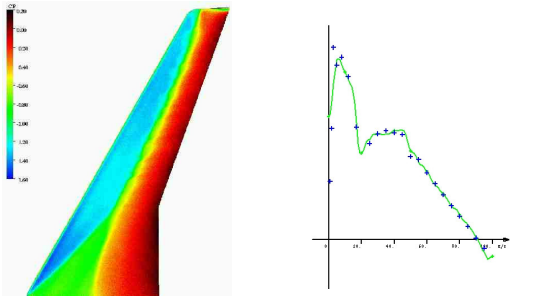

Fig. 7: PSP measurements compared to pressure taps measurements (PSI) on a half-wing in S2MA

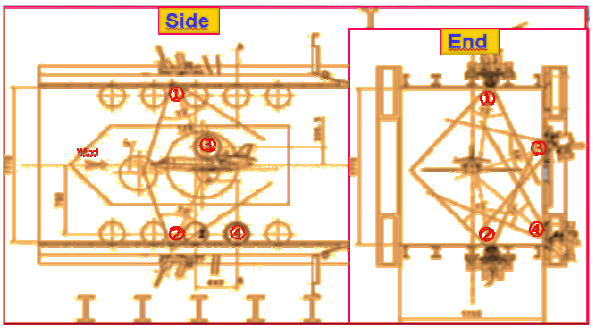

Fig. 8: "360°" PSP measurements with 4 cameras on a full aircraft model in S2MA

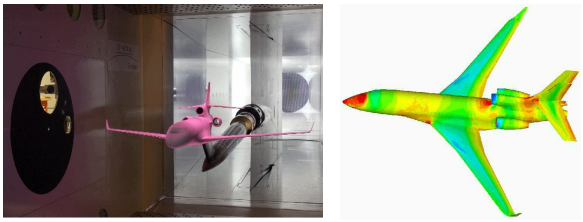

Fig. 9: PSP measurements on a full aircraft in S2MA

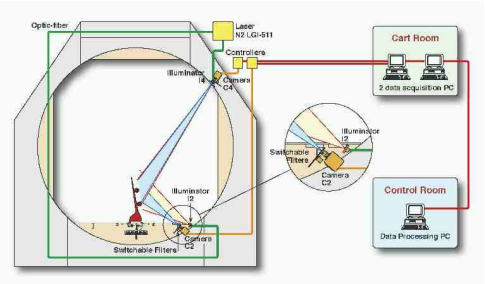

Fig. 10: PSP measurements in the large S1MA test section

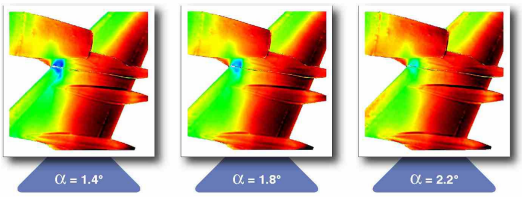

Fig. 11: PSP measurements on wing-nacelle in S1MA

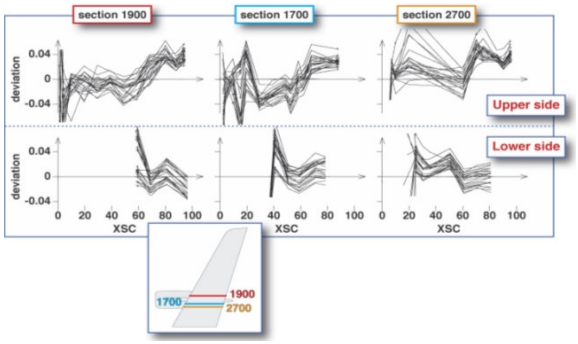

Fig. 12: Comparison of PSP measurement and pressure tap results on half-wing sections in S1MA

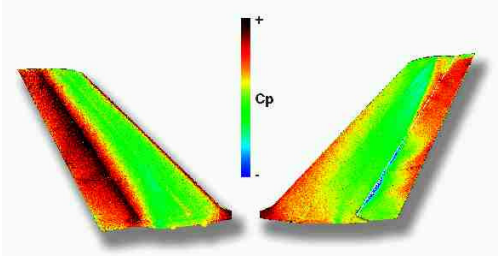

Fig. 13: PSP measurement on deflected rudder in S1MA

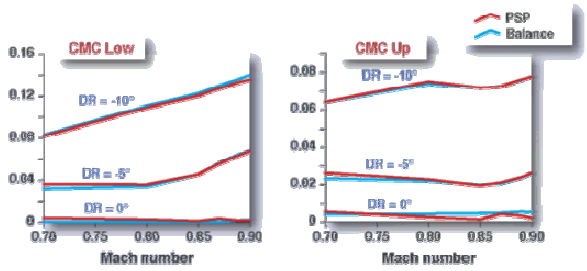

Fig. 14: Rudder efficiency from integrated PSP measurement compared to balance results in S1MA

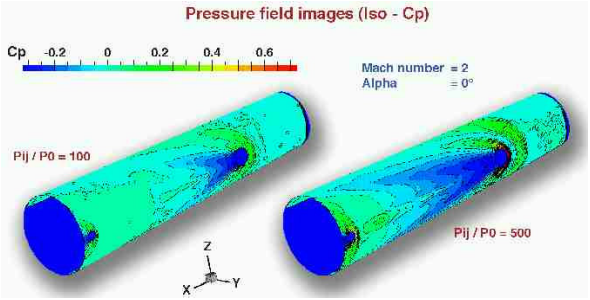

Fig. 15:PSP measurement of side-jet interaction on a missile fuselage in S3MA at M=2

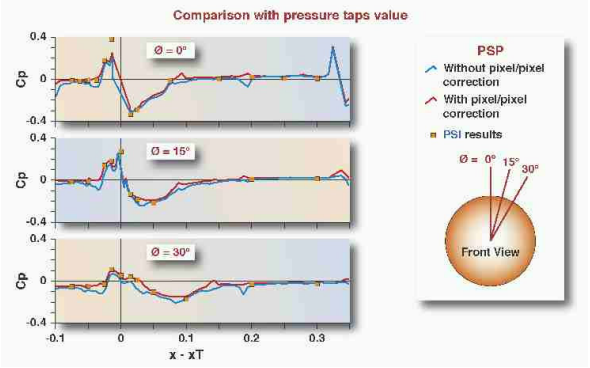

Fig. 16 :PSP measurement of side-jet interaction at different azimuth positions on a missile fuselage (M=2)

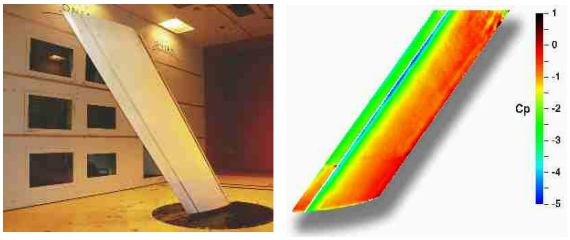

Fig. 17: Development of low speed PSP : upper surface pressure on a swept half-wing with deflected flaps in F1

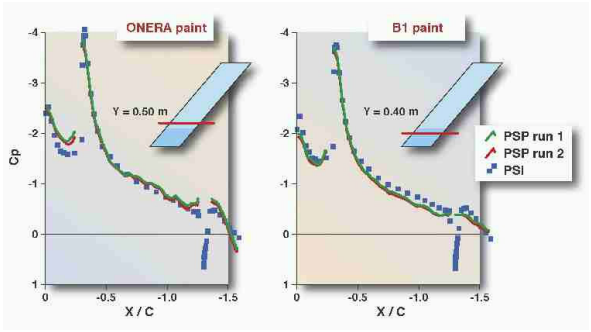

Fig. 18: PSP and pressure tap measurements on a swept half wing in F1 (M=0.25 ; pi=2.5 bar)

Fig. 19: Aircraft model to study wake survey in F1 wind tunnel by different techniques (5 holes probe, PIV, DGV)

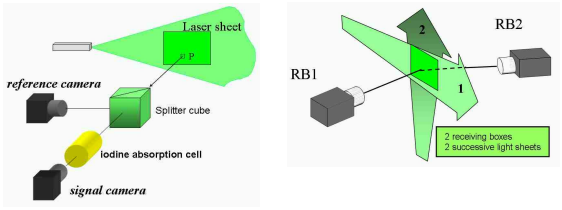

Fig. 20: DGV principle (left) and selected configuration with 2 reception boxes and 2 successive light sheets for the F1 test (right)

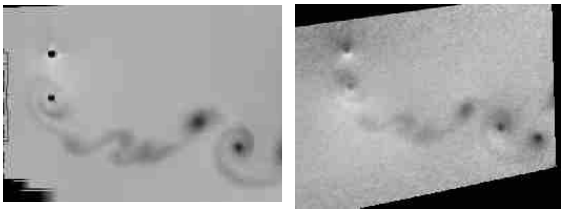

Fig. 21: Axial velocity field downstream of the wing as measured by 5 holes probe (left) and DGV (right)

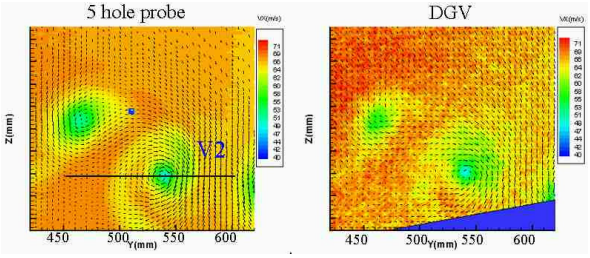

Fig. 22: Detail of the aileron contrarotating vortices : colors for axial velocity, vectors for in plane components

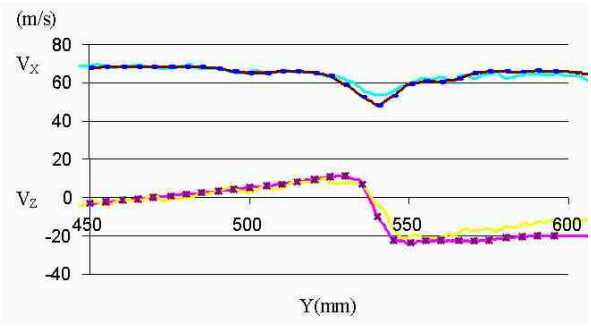

Fig. 23: Velocity downstream of the wing as measured by DGV and 5 holes probe

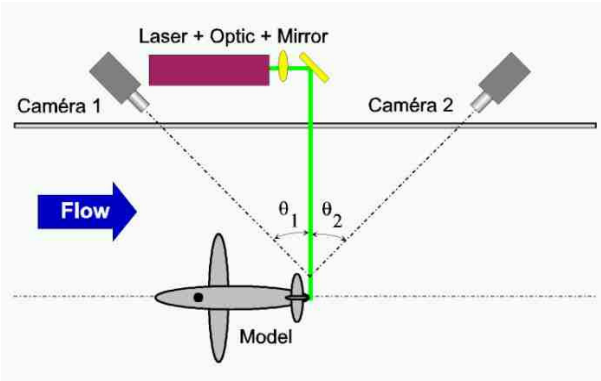

Fig. 24: 3C PIV arrangement in F1 wind tunnel

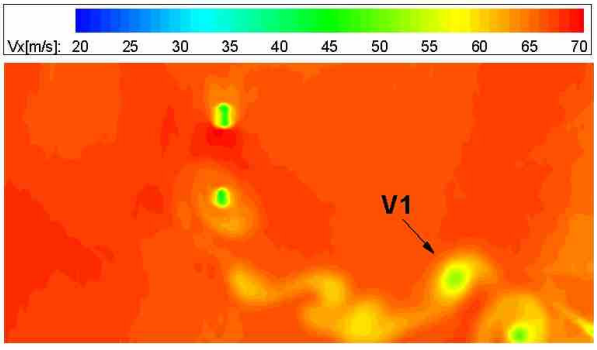

Fig. 25: Axial velocity component downstream of the wing as measured by PIV (aileron vortex named V1)

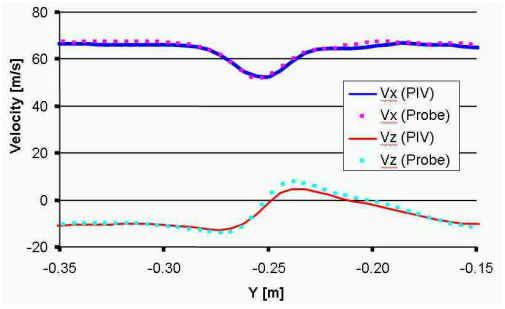

Fig. 26: Velocity downstream of the wing as measured by PIV and 5 holes probe

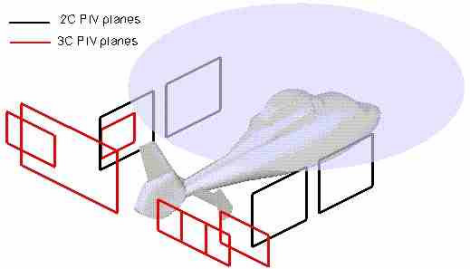

Fig. 27: PIV measurement planes around the Dauphin helicopter model in F1 wind tunnel (PIV measurements phased by the main rotor blades position)

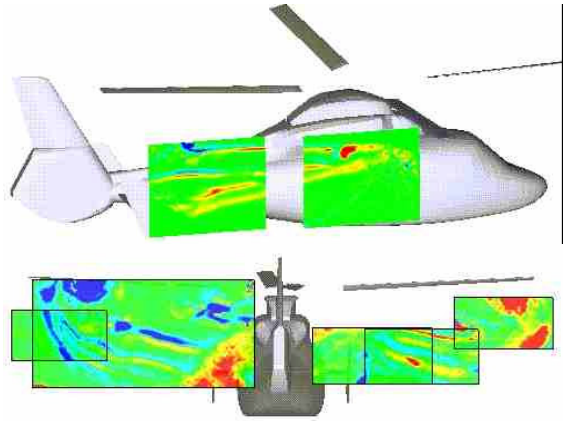

Fig. 28: Vorticity contours in the main rotor wake measured by PIV (side view : 2C PIV ; lower view from back : 3C PIV)

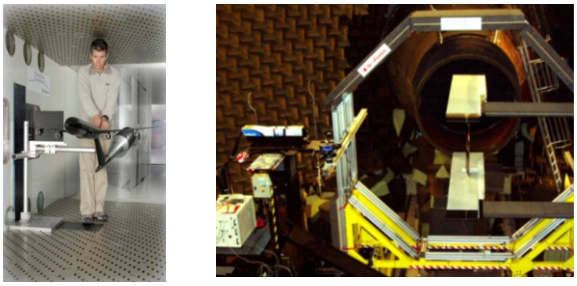

Fig. 29: New PIV system in the transonic S2MA (left) and in the anechoic CEPRA19 (right) wind tunnels